Electronic Supplementary Material (ESI) for Nanoscale.

Supporting Information

Polyethylene Oxide Film Coating Enhances Lithium Cycling Efficiency of an Anode-free Lithium Metal Battery

Addisu Alemayehu Assegie[a], Ju-Hsiang Cheng[a], Li-Ming Kuo[a], Wei-Nien Su[b], Bing-Joe Hwang[a,c*]

[a]Department of Chemical Engineering and [b]Graduate Institute of Applied Science Technology, National Taiwan University of Science and Technology, Taipei 10607, Taiwan.
[c]National Synchrotron Radiation Research Center (NSRRC), Hsinchu 30076, Taiwan.

* Corresponding author: bjh@mail.ntust.edu.tw

Thin film fabrication by spin coating can be controlled by solution concentration, spinning speed, viscosity of solvent, spinning duration and volume of solvent. Therefore, as the thickness of film is influenced by all these parameters, we optimize our electrode fabrication by dissolving a 0.1 gm Polyethylene oxide (PEO, molecular weight ~ 8 x10^6 g/mol) in equivalent mixture of water/ethanol and stirred for 12 hr using magnetic stirrer. After coating copper with spinning speed of 4000 rpm and spinning duration 120 sec optimal PEO film thickness 200 nm was obtained based on lithium cycling ability. Figure S1 and Table S1 shows thickness of PEO film obtained by varying the spinning speed.

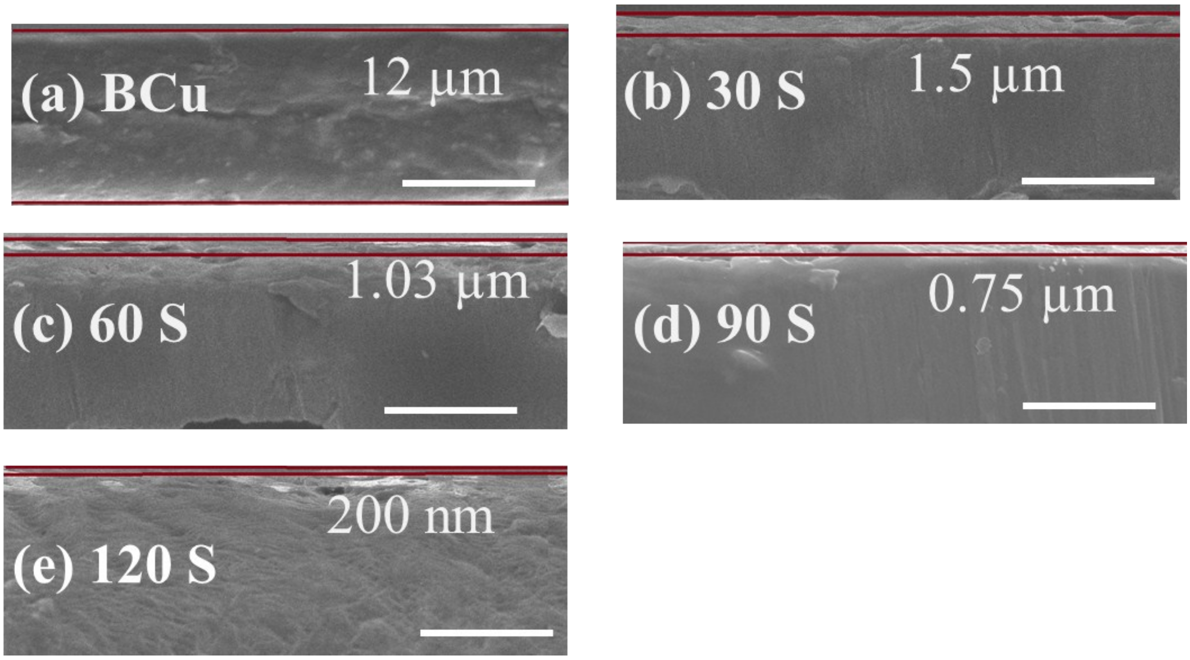

Figure S1. SEM cross section of bare and PEO modified electrode. (a) Bare copper, and (b-e) PEO modified copper electrodes (Cu@PEO), PEO film coated with spin coating speed 4000 rpm and duration of spinning time 30, 60, 90, and 120 seconds respectively. The scale bar represents 10 μm.

Table S1. Spinning/ coating time duration effect in Li/Cu@PEO cell Performance in 1M LiTFSI, DME/DOL (v/v 1/1), and 2 wt % $LiNO_3$ electrolyte.

Speed(rpm)	Spinning duration/time (S)	PEO/Film thickness (µm)	Average100 cycle CE (%)	Comment
Bare Cu	Nil	Nil	67	control
4000	30	1.50	78	
4000	60	1.03	82	
4000	90	0.75	95	
4000	120	0.20	~100	Average CE(%) ~100% due to activation of dead lithium

PEO modified electrode coated with spinning speed 4000 rpm and 120 sec with uniform top view (Figure S2a) and corresponding EDS mapping peak of copper substrate due to SEM energy penetration of coating layer. Figure S2b reveals carbon and oxygen peaks from PEO coating layer and their percentage composition is shown in Figure S2c. Figure S2d and Figure S2e show the bare and PEO modified copper contact angles, 47^o and 20^o respectively, measured with 1M LiTFSI, DME/DOL (v/v 1/1), and 2wt% $LiNO_3$ electrolyte. The low contact angle for modified electrode confirms the better wettability and compatibility of ether electrolyte with PEO coating layer. In contrast, the bare electrode gives a high contact angle due to the poor interaction of non-uniform bare electrode surface with electrolyte.

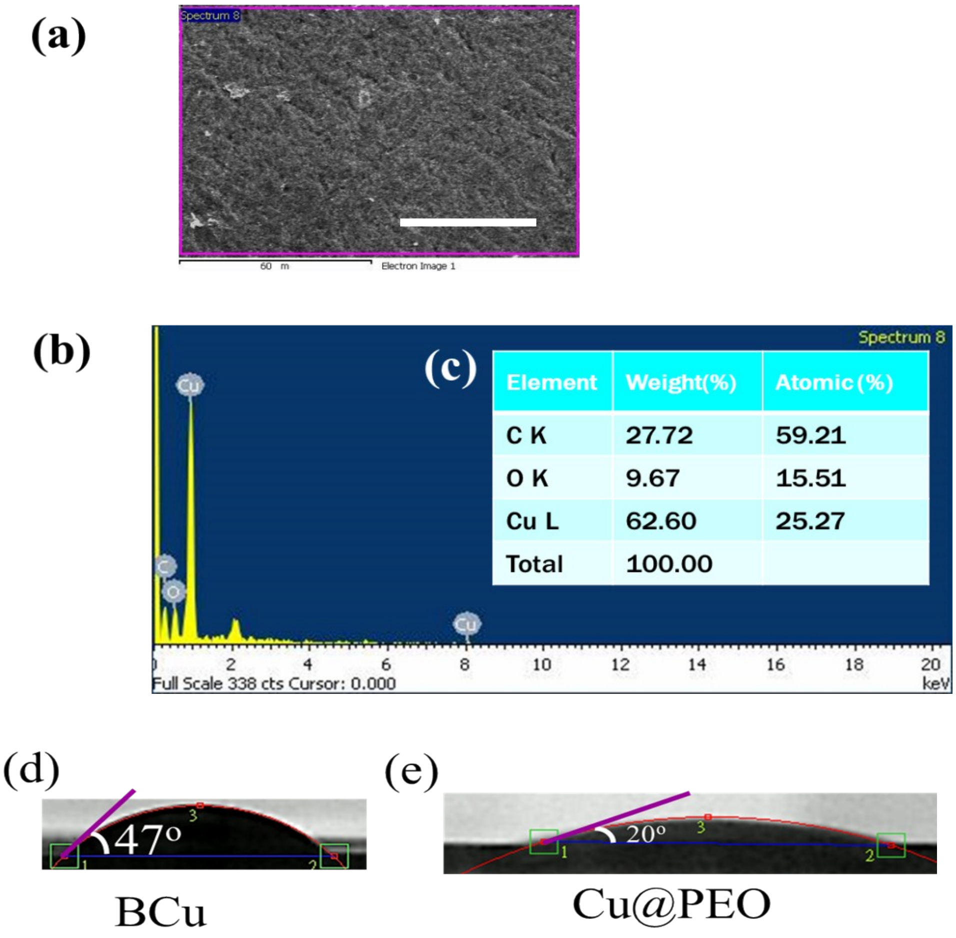

Element	Weight(%)	Atomic(%)
C K	27.72	59.21
O K	9.67	15.51
Cu L	62.60	25.27
Total	100.00	

Figure S2. PEO coated electrode with optimized thickness (a) SEM morphology of PEO modified electrode (10 µm) (b) Corresponding EDS of modified electrode (c) Elemental composition (inset) of modified film surface coated with spinning speed 4000 rpm and spinning time 120 sec. Contact angle measurements for (d) bare and (e) PEO modified electrodes with 1M LiTFSI, DME/DOL (v/v 1/1), 2 wt% $LiNO_3$

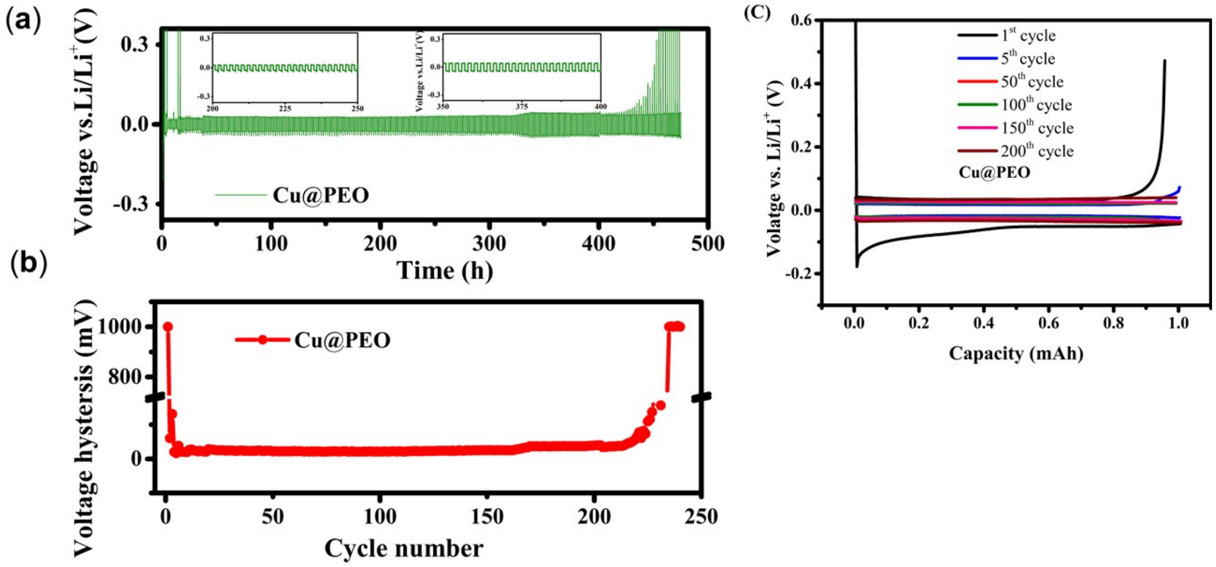

Figure S3. Long cycle performance of modified copper electrode (optimized) with lithium as reference and counter electrode (a) voltage profile (b) voltage hysteresis (c) selected cycle's voltage profile with current density of 0.5 mA cm^{-2} and lithium deposition capacity of 0.5 mAh cm^{-2} with 1M LiTFSI, DME/DOL (v/v 1/1), 2 wt% $LiNO_3$. Modified electrode with optimum coating conditions, 4000 rpm and 120 sec.

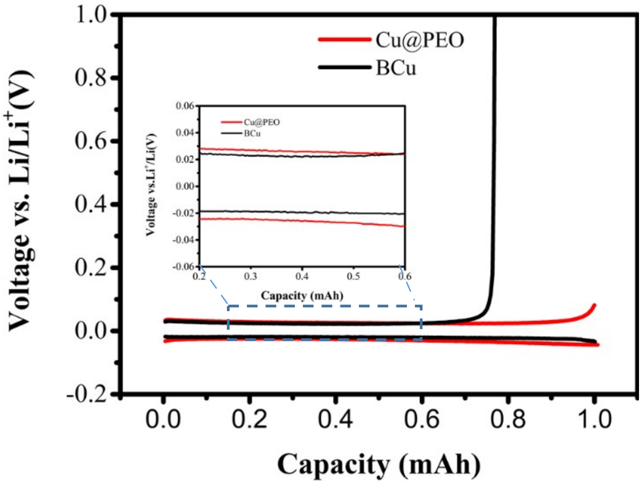

Figure S4. The voltage profiles of bare and PEO coated electrodes from the 5th cycle during the lithium deposition and stripping process, with Li metal as reference and working electrode at 0.5 mA cm^{-2} with 1M LiTFSI, DME/DOL (v/v 1/1), 2 wt% $LiNO_3$. Inset represents the enlarged capacity range from 0.2 to 0.6 mAh. Modified electrode with optimum coating conditions, 4000 rpm and 120 sec.

Figure 5Sa compares the Coulombic efficiency of bare and modified electrode in carbonate electrolyte. PEO coating also improve lithium cycling in comparison to bare electrode. However, lithium cycling ability of PEO modified electrode in carbonate electrolyte were inferior compared to ether based electrolyte since fluoride ion generated from decomposition of $LiPF_6$ reacts with PEO and rupture it. Coulombic efficiency failure after 50th cycle confirms total PEO film rupture and its inability to withstand lithium dendrite. Figure S5b and S5c show selected cycle's voltage profiles for control and modified electrodes in carbonate electrolyte. For the bare electrode, its 1st cycle charge capacity is higher than its subsequent value in the 5th cycle, possibly due to dendrite formation and higher resistance intensification. Bare electrode rapid capacity fading and large polarization with cycling results from aggressive lithium dendrite nucleation and unstable thick SEI layer formation. In contrast, the voltage profile curve of the modified electrode in Figure S5C shows higher charge capacity in its 5th cycle than the 1st cycle. The effect of capacity retention remains higher than 1st cycle for more than the first ten cycles due to efficient prevention of lithium dendrite by PEO film at this stage of cycling. However, with an increase in cycle number the PEO film were unable to tolerate lithium dendrite penetration.

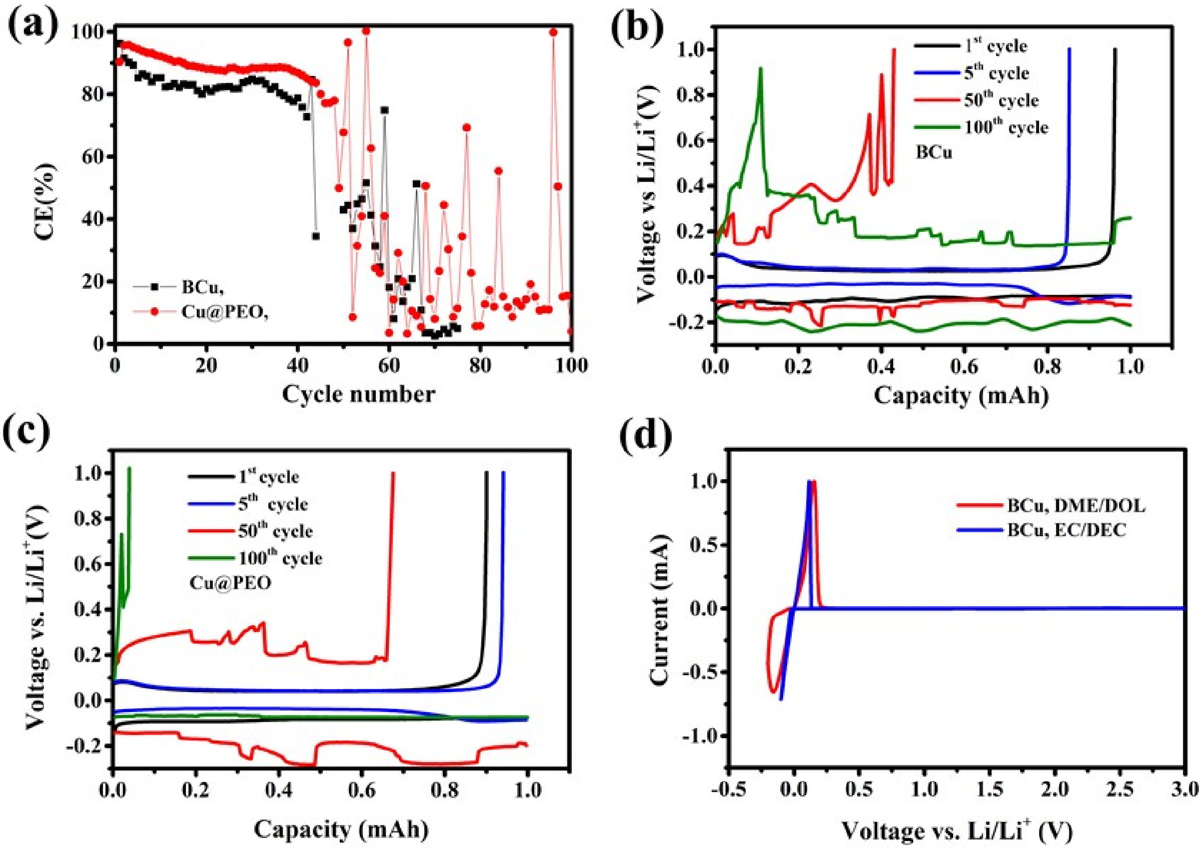

Figure S5. Cycling performance of bare copper and modified copper electrodes (a) CE(%), (b) voltage profile of BCu, (c) voltage profile of Cu@PEO electrode, with 1M LiPF$_6$, EC/DEC(v/v 1/1) electrolyte, E-range -0.5 V and J = 0.5 mA cm^{-2} and (d) Normalized cyclic voltammetry of Li-Cu cell with two electrolyte at scan rate of 0.5 mV S^{-1}.

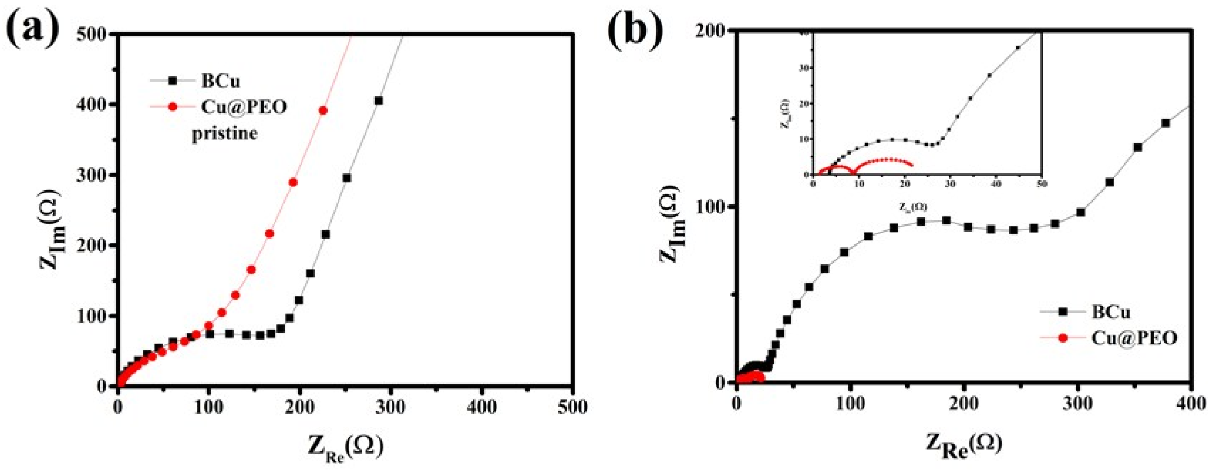

Figure S6. EIS for bare (BCu) and modified electrode (Cu@PEO) (a) Pristine (b) after 10th cycle with lithium as reference and counter electrode in 1M LiTFSI, DME/DOL (v/v 1/1), 2wt% $LiNO_3$ electrolyte. Modified electrode with optimum coating conditions, 4000 rpm and 120 sec.

Figure S7a and S7b show SEM morphology of bare and modified electrodes measured after 100 charge/discharge cycles in carbonate electrolyte. Both electrodes shows needle like lithium dendrite growth on copper electrode. The failure to control lithium dendrite nucleation and growth in PEO modified electrode shows incompatibility of the polymer with $LiPF_6$, EC/DEC electrolyte. Figure S7c shows modified electrode dendrite free morphology after 200 charge/discharge cycles in ether based electrolyte run at higher rate (1 C).

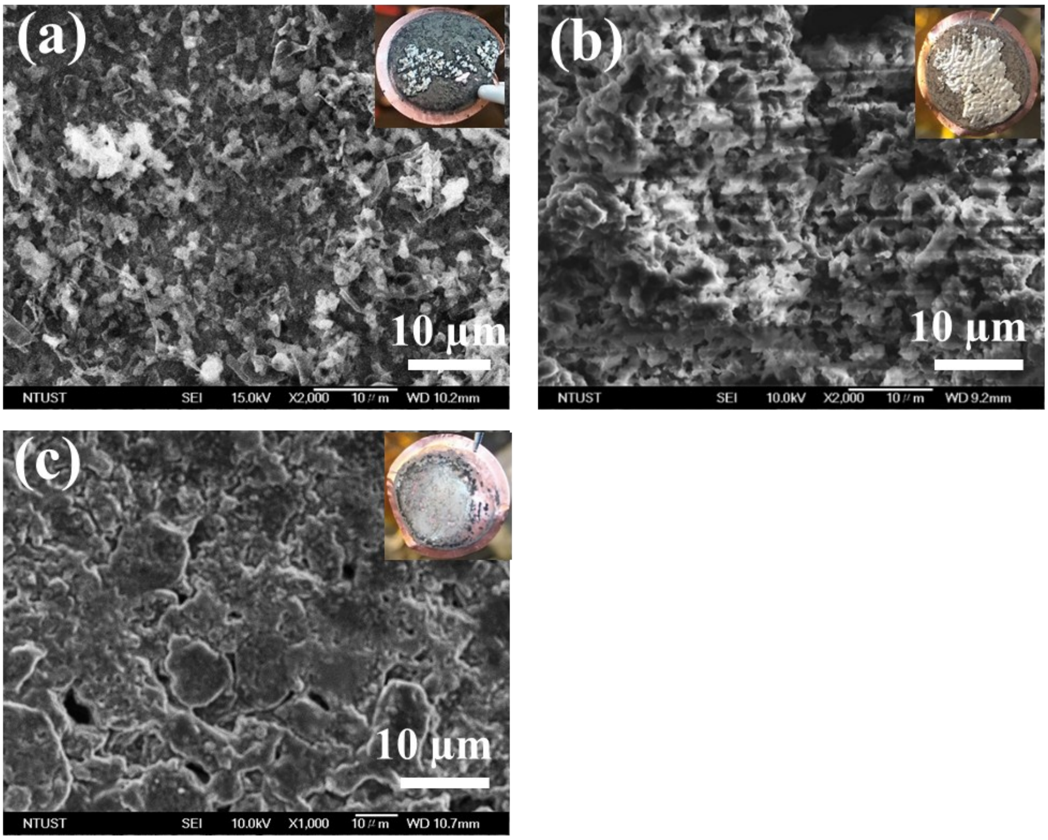

Figure S7. Bare and modified copper optical images (inset) and SEM morphology of deposited lithium after cycling with lithium as reference and counter electrode. (a)BCu, (b) Cu@PEO after 100 cycles in 1M $LiPF_6$, EC/DEC (v/v 1/1), (c) Cu@PEO after 200 cycle in 1M LiTFSI, DME/DOL (v/v 1/1), and 2 wt% $LiNO_3$ with a current density of 0.5 mA cm^{-2}.

Table 2. Cyclic voltammetry of three cells and their redox peak current and potential measurement for three cells

Cell type	Cycle number	E_a/E_c (V)	I_{pa}/I_{pc} (mA)	E (mV)
Li/LFP	1	3.64/3.23	2.90/-2.62	410
	2	3.64/3.23	2.88/-2.61	410
	3	3.64/3.23	2.88/-2.56	420
BCu/LFP	1	3.63/3.26	1.86/-1.56	370
	2	3.64/3.24	1.98/-1.63	400
	3	3.64/3.24	1.94/-1.57	400
Cu@PEO/LFP	1	3.61/3.27	2.44/-2.02	340
	2	3.61/3.27	2.88/-2.27	340
	3	3.61/3.27	2.87/-2.33	340

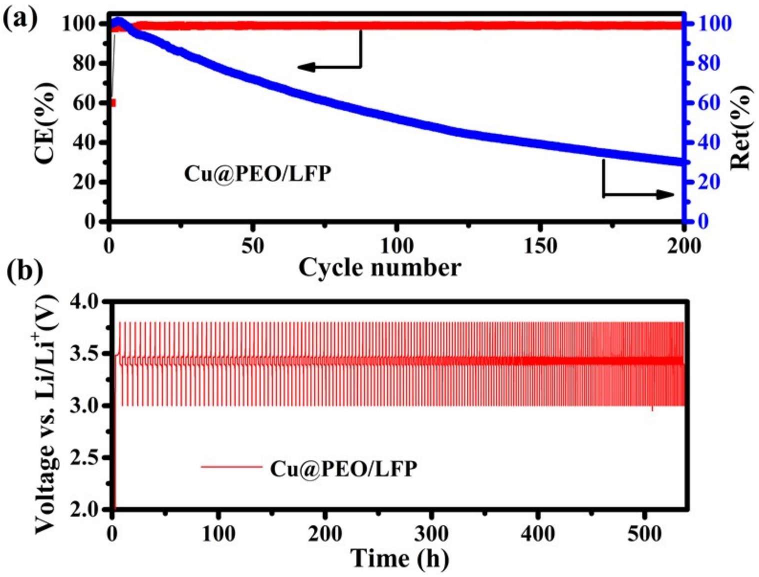

Figure S8. Long cycle performance of Cu@PEO/LFP, full cell (a) CE (%) and capacity retention (%); (b) Corresponding voltage profile at 0.2 C in 1M LiTFSI, DME/DOL (v/v 1/1) and 2 wt% $LiNO_3$, E-range 3.0-3.8V.

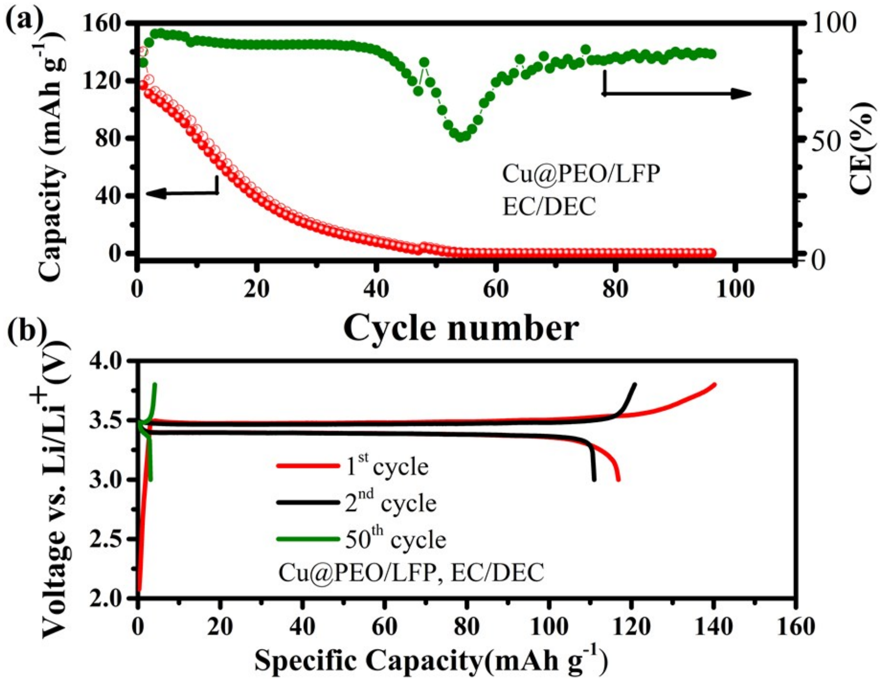

Figure S9. Cycling performance of modified electrode, Cu@PEO/LFP, anode free full cell (a) Capacity & CE (%) vs cycle number. (b) Voltage profile of anode free battery in 1M $LiPF_6$, EC/DEC (v/v 1/1) and electrolyte, E-range 3.0-3.8 V and at 0.2 C rate.

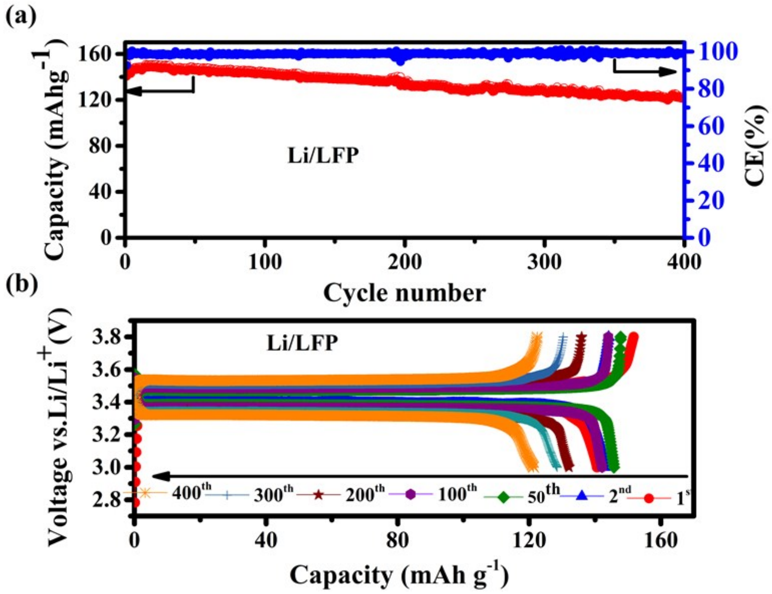

Figure S10. Li/LFP cell (a) Electrochemical cycling performance. (b) Galvanostatic charge/discharge curves in1M LiTFSI, DME/DOL, (v/v 1/1), 2 wt% $LiNO_3$ electrolyte, E-range 3.0-3.8V and 0.1 C rate.

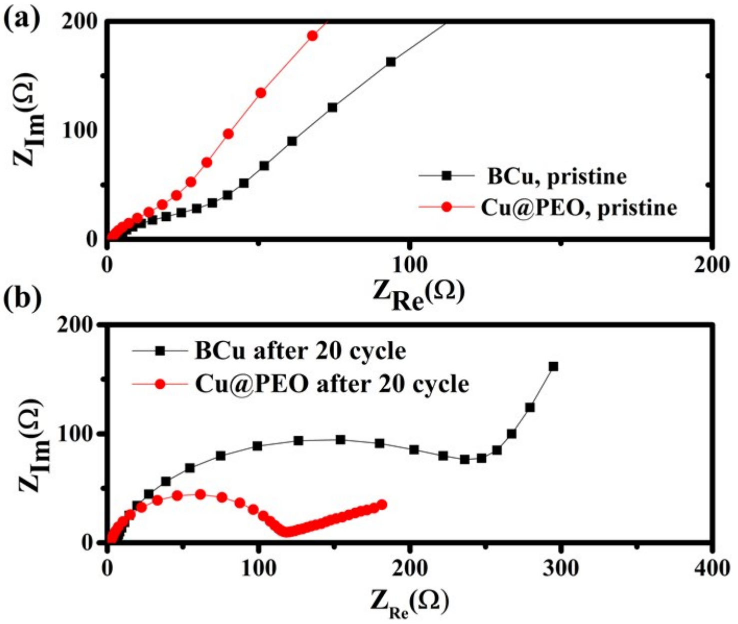

Figure S11. EIS for anode free full cells ((BCu/LFP) and Cu@PEO/LFP)). (a) Pristine (b) after 20th cycle with in 1M LiTFSI, DME/DOL (v/v 1/1), and 2 wt% $LiNO_3$ electrolyte. All cells cycled with 0.2 C rate and data collected at discharge state.

Atomic force microscope (AFM) is essential for studying surface roughness (or average deviation) at the nanoscale, having resolution far exceeding that of optical based methods. The measured roughness of any given surface depends on both the spatial and vertical resolution of the instrument. This is because real surfaces exhibit roughness on many length scales and can be thought of as a superposition of these profiles.

Detailed PEO films surface structures observed by AFM are shown in Figure S12. To clearly confirm PEO film relative smoothness, AFM measurement were conducted on films obtained with the same coating procedure on the copper substrate, as described in experimental method. 2D and 3D surface micrographs of PEO films prepared by different spinning time were measured. As seen in Figure S12a, the film obtained with spinning time of 120 s is much uniform compared with the film coated with spinning time of 90 s (Figure S12b) . Moreover, their corresponding roughness measurement 55 nm (120 s) and 95.4 nm (90 s) confirms that the film prepared under the optimal conditions exhibits a relatively smoother surface.

We also investigate whether the surface roughness of PEO film was affected by the nature of substrate. Effect of substrate was clearly demonstrated by coating PEO film on a much uniform silicon wafer substrate under the same conditions (spinning speed of 4000 rpm and coating time of 120 s). In this case, the roughness profile decreased greatly to 6.85 nm.

Thus we can conclude that PEO film roughness decreases with an increase in coating time and is also dependent on substrate nature, based on AFM and SEM morphology results.

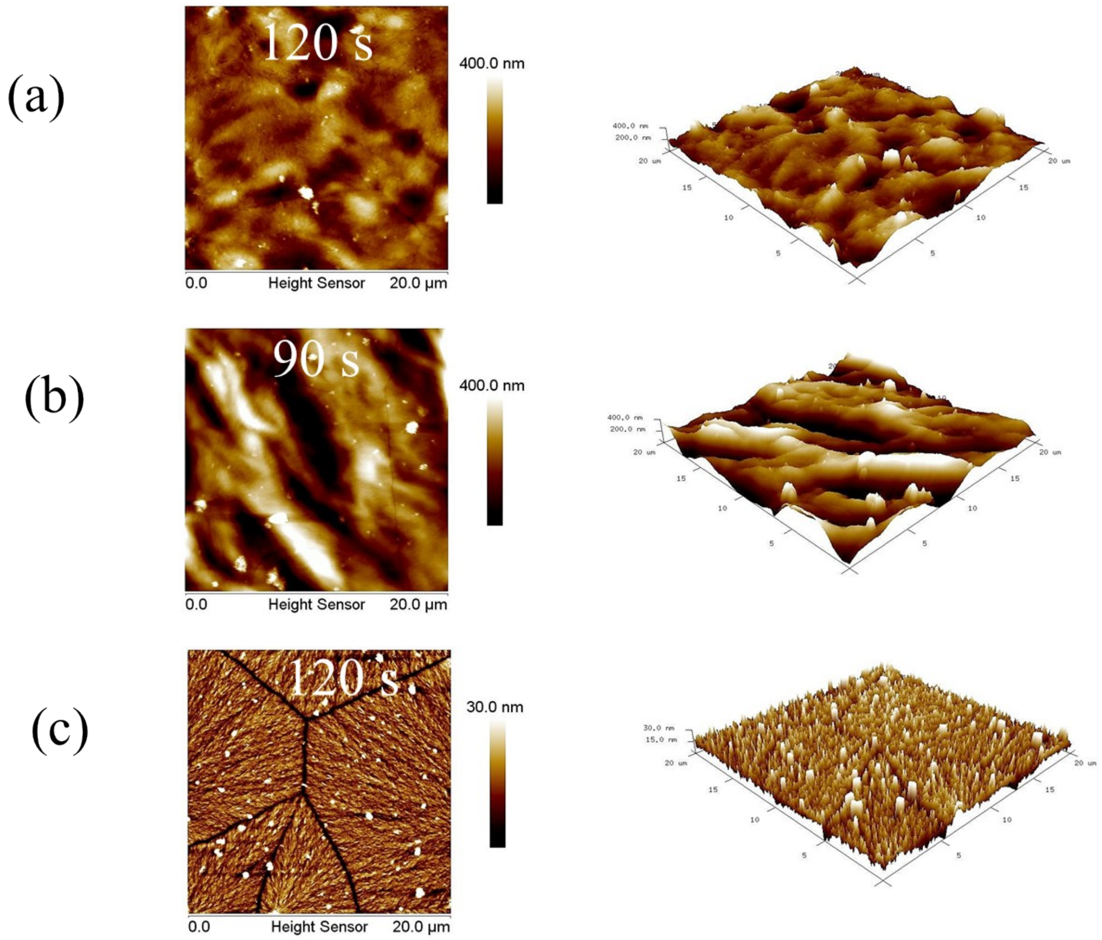

Figure S12. The AFM micrograph of PEO film coated on copper (a) 120 s, (b) 90 s coating times and (c) silicon wafer 120 s. AFM images 2D (left) and 3D (right) surface analysis of PEO film. All substrates coated with spinning speed of 4000 rpm.